PROTEINS: Structure, Function, and Genetics 16:364–383 (1993)

Crystal Structure of *Escherichia coli* TEM1 β-Lactamase at 1.8 Å Resolution

Christian Jelsch,[1,2] Lionel Mourey,[1,2] Jean-Michel Masson,[3] and Jean-Pierre Samama[1,2]

[1]Groupe de Cristallographie Biologique, Laboratoire de Pharmacologie et de Toxicologie Fondamentales, 31077 Toulouse, France; [2]UPR de Biologie Structurale, Institut de Biologie Moléculaire et Cellulaire du CNRS, 67084 Strasbourg, France; and [3]Groupe Ingénierie des Protéines, Laboratoire de Pharmacologie et de Toxicologie Fondamentales, 31077 Toulouse, France

ABSTRACT **The X-ray structure of *Escherichia coli* TEM1 β-lactamase has been refined to a crystallographic *R*-factor of 16.4% for 22,510 reflections between 5.0 and 1.8 Å resolution; 199 water molecules and 1 sulphate ion were included in refinement. Except for the tips of a few solvent-exposed side chains, all protein atoms have clear electron density and refined to an average atomic temperature factor of 11 Å^2. The estimated coordinates error is 0.17 Å. The substrate binding site is located at the interface of the two domains of the protein and contains 4 water molecules and the sulphate anion. One of these solvent molecules is found at hydrogen bond distance from S70 and E166. S70 and S130 are hydrogen bonded to K73 and K234, respectively. It was found that the *E. coli* TEM1 and *Staphylococcus aureus* PC1 β-lactamases crystal structures differ in the relative orientations of the two domains composing the enzymes, which result in a narrowed substrate binding cavity in the TEM1 enzyme. Local but significant differences in the vicinity of this site may explain the occurrence of TEM1 natural mutants with extended substrate specificities.**

Key words: X-ray structure, TEM1, β-lactamase, antibiotics, bacterial resistance, serine hydrolase

INTRODUCTION

β-lactamine molecules are the most commonly used antibiotics in antibacterial therapy. Their targets are the penicillin-binding proteins (PBPs), inner-membrane carboxy-transpeptidase enzymes involved in the biosynthesis and repair of the bacterial cell wall. However, the therapeutic effectiveness of β-lactam antibiotics is constantly diminishing. This bacterial resistance is mainly due to the β-lactamase enzymes that protect the bacterial carboxy-transpeptidases by hydrolyzing the β-lactam ring before the antibiotics reach their targets.

Genes coding for β-lactamases are proliferating among pathogenic bacterial strains in hospitals. For instance, the TEM enzyme, encoded on a plasmid in *Escherichia coli*, is widespread among numerous species of Gram$^-$ bacteria. Newly introduced antibiotics rapidly lose their therapeutic effectiveness as β-lactamases acquire the ability to hydrolyze them. It appears that these enzymes, under intense antibiotic pressure on bacteria, extend their hydrolysis spectrum through point mutations of amino acids. Several TEM and SHV derived β-lactamases, which confer bacterial resistance to the third generation cephalosporins, notably cefotaxime and ceftazidime, have been recently identified.[1–3]

Various classifications of β-lactamases have been proposed. The sequence alignment approach divides β-lactamases in 4 classes: A, B, C, and D.[4,5] Many class A β-lactamases from Gram$^+$ organisms are penicillinases. The TEM and SHV class A β-lactamases, disseminated in Gram$^-$ bacteria, hydrolyze both penicillins and cephalosporins.[6] Class C β-lactamases have a cephalosporinase substrate profile. Enzymes hydrolyzing oxacillin more efficiently than penicillin have been grouped in class D. Various crystal structures of wild-type class A β-lactamases have been reported: *Streptomyces albus* G,[7] *Staphylococcus aureus* PC1,[8] *Bacillus licheniformis* 749/C,[9] *E. coli* TEM1,[10] as well as protein mutant structures: D179N of *S. aureus*[11] and E166A of *B. licheniformis*.[12] Independently of our work, X-ray analysis of the TEM1 E166N mutant-PenG complex has recently appeared.[13]

Despite their high sequence homologies and the similarities in their three-dimensional structures, the class A β-lactamases demonstrate different catalytic efficiencies toward penicillin and cephalosporin antibiotics[14] which should be explained by differences in the protein structures. Hydrogen bond networks, which provide long-range interactions, are observed in the 1.8 Å resolution TEM1 structure. The significant differences observed between

Received January 7, 1993; revision accepted March 19, 1993.

Address reprint requests to Pr. J.P. Samama, Groupe de Cristallographie Biologique, Laboratoire de Pharmacologie et de Toxicologie Fondamentales, CEMES-CNRS, 29 rue Jeanne Marvig, BP4347, 31055 Toulouse, France.

TABLE I. Fast Rotation Function as a Function of the Resolution Range*

	Upper resolution limit					
δ/σ†	3.5 Å	4 Å	4.5 Å	5 Å	6 Å	7 Å
Lower resolution limit						
20 Å	1.54	1.33	1.00	0.86	1.07‡	1.13‡
15 Å	0.92	0.67	0.48	0.40	0.55‡	0.72‡
12 Å	0.65	0.67	0.30	0.16	0.34‡	0.50‡
10 Å	0.10	0.01	2nd position	2nd position	4th position	Absent
8 Å	Absent	Absent	Absent	Absent	Absent	—

*Normalized structure factors E were used; the Patterson cutoff was 4–30 Å.
†The value δ/σ represents the difference between the right peak and the next highest peak divided by the standard deviation. The first peak corresponds to the right solution unless stated.
‡The maximum of the rotation function duplicates in two near maxima. Euler angles of the rotation function solution are: α = 171°, β = 75°, γ = 168°.

TEM1 and PC1 are certainly linked to the different catalytic behaviors and to the evolution of substrate specificity capability.

MATERIALS AND METHODS

Crystallization, Data Collection, and Structure Determination

Crystals of *E. coli* β-lactamase TEM1 were prepared by the hanging drop method at 6°C. A solution of protein (20 mg/ml) in 10% saturated ammonium sulphate solution, 60 mM phosphate buffer at pH 7.8, was equilibrated against the same buffer containing 46% ammonium sulphate and 4% (v/v) acetone. The crystals diffract up to 1.8 Å resolution and belong to space group $P2_12_12_1$ with cell dimensions a = 43.1 Å, b = 64.4 Å, c = 91.2 Å. There is one molecule per asymmetric unit.[15]

Diffraction data were measured on a Siemens/Nicolet area detector with monochromated CuKα X-rays supplied by a Rigaku anode generator. Five crystals were used and a unique set of structure factors containing 98% of the possible reflections at 1.8 Å resolution was obtained. Ninety-eight percent of the reflections have a signal/noise ratio ($F/\sigma F$) greater than 5.0.

Structure determination using the molecular replacement method with a polyalanine model derived from the Cα coordinates of PC1 β-lactamase[16] (Protein Data Bank entry: 1BLM) turned out to be possible. The best signal of the fast rotation function[17] was obtained using a large resolution range (20–3.5 Å). Inclusion of low resolution data (20–12 Å) was essential to observe the right peak in the first position (Table I). The solutions from the translation function of Crowther and Blow,[18] performed between 4–20 Å resolution, were checked by visual inspection on computer graphics of the resulting crystal packing. The right translation was definitely discriminated by rigid-body refinement between 10 and 7.0 Å resolution using the program CORELS[19] and was best identified according to the correlation coefficient computed between F_{obs} and F_{calc}. According to this criteria, the difference between correct and wrong translation solutions amounted to 9% but was only 1.5% according to the R value calculation. The molecular replacement model, including side chain atoms, was partly refined using CORELS and energy minimization with X-PLOR[20] to a crystallographic R-factor of 0.39 between 10 and 3.5 Å resolution. The set of phases calculated from this model was used to interpret the four heavy atom derivatives that were found at that time: K_2PtCl_4, parachloromercury benzene sulfonic acid (PCMBS), K_2HgI_4, and $KAu(CN)_2$. The multiple isomorphous replacement (MIR) method provided an electron density map of good quality at 3.5 Å resolution (f.o.m. = 0.71), which was further improved by solvent flattening. The protein was built in this electron density map. The crystal structure determination and refinement at 2.5 Å resolution has been previously reported.[10]

Crystallographic Refinement

Molecules and electron density maps were displayed on an Evans and Sutherland ESV3+ interactive graphic system using the program FRODO.[21] The X-PLOR package version 2.1 was used for refinement in reciprocal space. Simulated annealing, with molecular dynamics, was run using the slow cooling protocol for 2.7 ps (time step of 0.5 fs) with decreasing temperature from 3,000°K to 300°K. Molecular dynamics simulations were followed by 150 cycles of energy minimization. Temperature factors were refined using the BGROUP option (two B factors per residue) in the first reciprocal space refinement at 2.9 Å resolution. In the following refinement cycles, individual atomic B factors were refined.

The resolution was extended in five steps from 2.9 Å to 1.8 Å. Manual corrections of the structure were done after each step, and eventually dealt with inappropriate atom shifts occuring during the computation. The unambiguous positioning of loop regions and the assignment of most amino acids were done, after the first refinement cycle (R = 0.267), in a $(m_{comb} \times F_{obs}, \Phi_{comb})$[22] electron density map com-

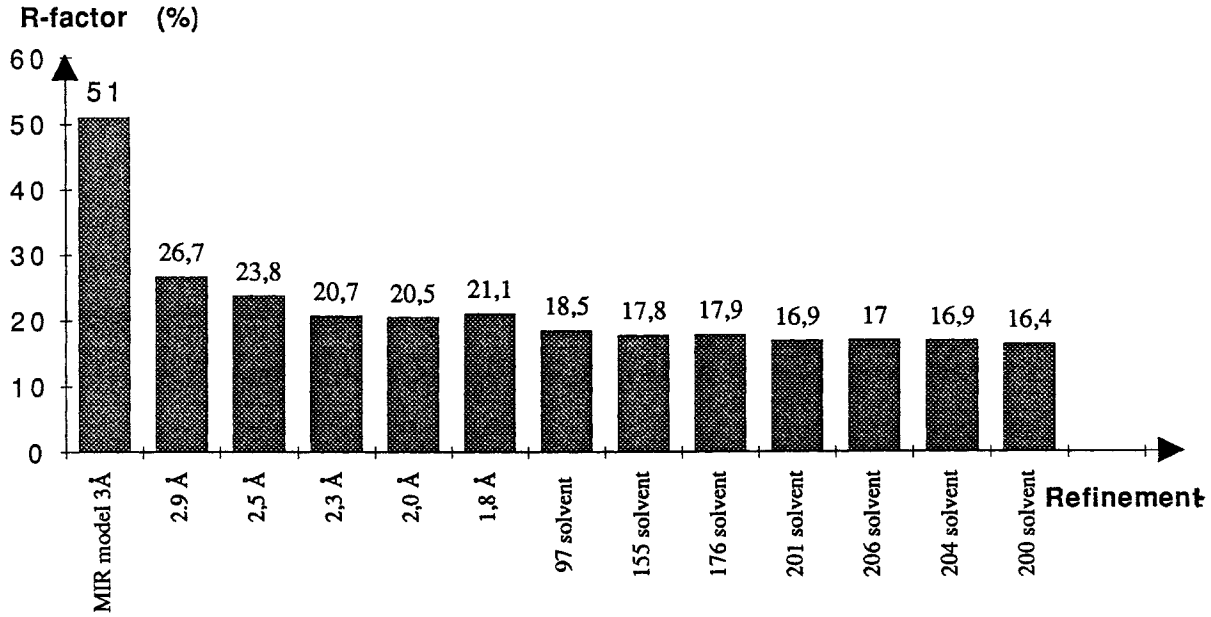

Fig. 1. Evolution of the crystallographic *R*-factor during refinement. The resolution shell and the number of solvent molecules included at each step are indicated.

puted at 2.9 Å resolution. After refinement, one sequence shift was corrected at 2.5 Å resolution, in a $(3F_{obs} - 2F_{calc}, \Phi_{calc})$ map. The proper orientation of some carbonyl groups and of the side chains of threonine and leucine residues were defined in the 2.3 Å and 2.0 Å resolution electron density maps. The protein structure was in excellent agreement with the $(2F_{obs} - F_{calc}, \Phi_{calc})$ electron density map computed at 1.8 Å resolution after the fifth refinement cycle, and solvent molecules handling was started at that stage.

Inclusion of Water Molecules

Water molecules were included so as to account for the largest positive peaks in the $(F_{obs} - F_{calc}, \Phi_{calc})$ difference Fourier map, drawn at four standard deviations above the mean electron density value, provided they were at hydrogen bond distance from protein or other solvent atoms. Isolated electron density peaks were ignored. Water molecules were introduced in seven steps, with initial occupancy and *B* factor respectively fixed to 0.8 and 20 Å^2. Molecular dynamics was not performed after incorporation of solvent molecules and atomic positions were only refined by energy minimization. Atomic temperature factor refinement was performed using the BREFINEMENT procedure of the X-PLOR package and the water occupancies were refined using the program PROLSQ.[23] During this process, water molecules were discarded when their temperature factors refined to more than 40 Å^2 or when their occupancies were less than 0.3.

Refinement converged as the number of solvent molecules reached 200. Occupancies and temperature factors were finally refined five times alternatively and successively. The water molecules have been sorted in descending order of reliability, where the reliability is defined by the quality factor: (occupancy)^2/(temperature factor).[24]

As a final stage of the refinement process, the histidine, asparagine, and glutamine side chains were examined and eventually reoriented in the electron density in order to satisfy appropriate and reasonable hydrogen bonding patterns.

RESULTS

Refinement

The evolution of the crystallographic *R*-factor during refinement is described in Figure 1. The *R*-factor of the initial model built in the solvent flattened MIR electron density map was 0.51. It dropped to 0.34 after energy minimization and reached 0.26 after molecular dynamics refinement, including data to 2.9 Å resolution. The resolution was extended in five steps to 1.8 Å and the *R*-factor did not cross the 0.20 barrier as long as water molecules were not included in the refinement.

After inclusion of the first set of 97 water molecules, the $(F_{obs} - F_{calc}, \Phi_{calc})$ electron density map displayed four positive peaks in a regular tetrahedral arrangement around an already present water molecule. This arrangement of atoms was interpreted as a sulphate anion, consistent with the fact that crystals were obtained in 46% saturated ammonium sulphate. Its position was assumed reasonable,

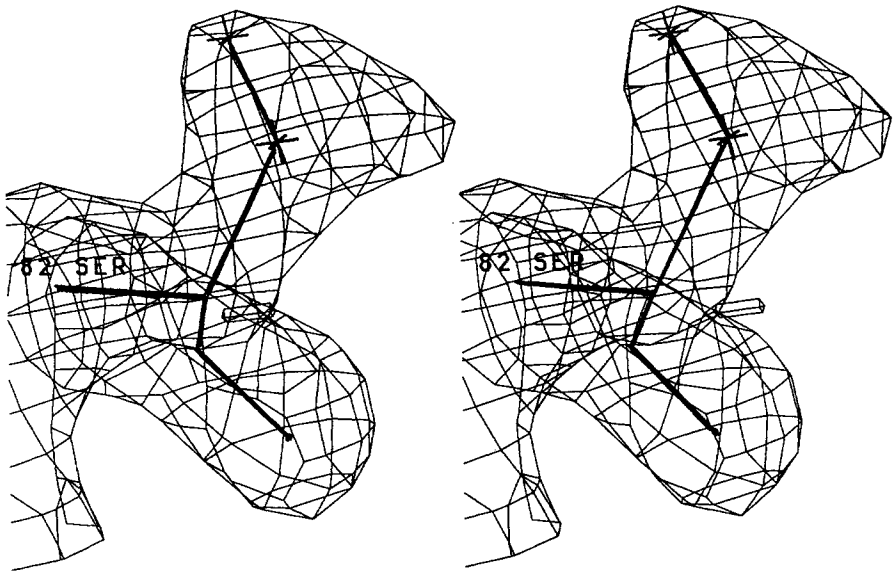

Fig. 2. Electron density map ($2F_{obs} - F_{calc}$, Φ_{calc}) at 1.8 Å resolution of residue Ser 82. The contour level is 1.0 σ.

in the vicinity of S130 and R244 side chains. Its occupation and temperature factor are 0.7 and 25 Å^2, respectively. Another feature of the difference Fourier map, was the presence of positive peaks near each hydroxyl group of S82 and S285. Both peaks were too close to the Cβ atom to be assigned to water molecules and were interpreted as the occurence of two alternate conformations of the serine side chains (Fig. 2).

The electron density is well defined for the whole protein except at the end of a few long side chains exposed to solvent. Consistently, those residues: K55, R83, Q88, Q90, Q99, E104, K111, K146, K256, and R277 have relatively high temperature factors (30 to 40 Å^2).

After convergence of the refinement at 1.8 Å resolution, all 263 amino acids of TEM1 β-lactamase, 199 water molecules, and a sulphate anion were assigned. The crystallographic *R*-factor is 0.164 for 22,510 reflections between 5 and 1.8 Å resolution. Average temperature factors and deviations from ideal geometry are given in Table II. The distribution of the *B* factors along the polypeptide chain is shown in Figure 3. The essential residues for catalysis (S70, K73, S130, E166, K234) have temperature factors below the average value computed for all protein atoms. The total water content in the crystal amounts to 43%. The Luzatti plot[25] gives an estimate of the coordinates error of 0.17 Å (Fig. 4). The Ramachandran plot (Fig. 5) reveals a few residues in medium to highly strained conformations: M69, S130, N175, D179, and L220. Their structural implications will be discussed.

Description of the Structure

The TEM1 enzyme (Fig. 6) is a globular protein of ellipsoidal shape with dimensions 30 Å × 40 Å × 50 Å. Its secondary structure elements were assigned using the program DSSP[26] (Table III). Seventeen percent of the residues are involved in β-strands, 5% in 3_{10} helices, and 39% in α-helices. The molecule can be described as a two domains protein. The first one includes a five-stranded β-sheet onto which helices H1, H10, and H11 are packed, toward the solvent interface. The interface between this β-sheet and the 3 helices is a large hydrophobic core. The second domain is made of eight helices (H2 to H9) located on the other side of the pleated sheet. Two hinge regions are connecting these domains which generate a large depression at their interface, corresponding to the substrate binding site. These hinge regions are held by hydrogen bonds and salt-bridges which should prevent any large conformational change to occur.

The main β-sheet is formed by five antiparallel strands (Fig. 7). The residues of the two first strands (S1 and S2) belong to the N-terminal part of the chain (43–60), and the three others (S3, S4, S5) to the C-terminal moiety (230–266). A β-bulge occurs, between β-strands S1 and S2, at position 58; according to the classical β-bulge nomenclature, L57, E58, and E48 are, respectively, at positions 1,2, and X of that motif.[27] In addition to the main β-sheet, there are two small two-stranded antiparallel sheets (SB and SC). Each strand is made of two residues.

Strand S2 (56–60) is made of five residues, while its adjacent strand S1 (43–50) is eight residues long.

TABLE II. Refinement Statistics and Deviations From Ideal Geometry

Resolution range	5–1.8 Å
R-factor for 22,510 reflections	16.4%
Average temperature factors	
Main chain atoms (Cα, N, C, O)	8.8 Å^2
Side chain atoms	13.1 Å^2
Water molecules	15.1 Å^2
Whole molecule (including solvent)	11.3 Å^2
Root-mean-square deviations from ideal geometry	
Bond lengths	0.019 Å
Angles	2.66°
Dihedral angles	23.1°
Improper dihedral angles	1.12°

As a consequence, residues 43 and 44 at the N-terminal end of S1 have no hydrogen bonding partners. This is compensated by the hydrogen bond, also found in the *B. licheniformis* enzyme, between V44 main chain nitrogen atom and E37 side chain and by the salt-bridge R43-E64 (Fig. 8). These interactions, together with the salt-bridge between R61 and E64 and the hydrogen bond between E37 and R61 side chains, form the first hinge region. It locks the N-terminal part of the interdomain crossover loop, made of residues 60–68, which links strand S2 to the catalytic helix H2.

The conformation of the second hinge region (residues 212–222, Fig. 9) is determined by the salt-bridge between R222 and the conserved and buried D233. A structural water molecule, WAT294, stabilizes the loop 217–220 and provides the missing hydrogen bond partners of main chain nitrogen atoms L221 and R222 at the N-terminal part of 3_{10} helix H10.

Topology of the Substrate Cavity

Several regions define this cavity shown in Figure 10: on one side, residues 234–237 belong to strand S3 while R244 is found on the adjacent strand S4. Residues E104 and Y105 are located in a solvent exposed loop before H3. The electron density of Y105 is weak and its side chain has relatively high atomic temperature factors (≈ 25 Å^2). S130, D131, N132, which form a short connection between helices H4 and H5, are on the opposite side of the cavity with respect to strand S3. D131 side chain is buried and interacts with the main chain nitrogen atoms of V108, T109, N132, T133, and A134, bringing strong constraints on the respective positions of the N termini of H3 and H5 to which these residues belong. In addition, it forms a hydrogen bond with T109OG1. This strong anchoring of D131 might insure the correct positioning of S130 and explains its slightly strained conformation. V216 side chain is pointing toward the cleft where the acylating S70 is located. According to the DSSP secondary structure assignment, this serine belongs to a one turn 3_{10} helix (69–71) continued by an α-helix (72–85) which brings K73 side chain at 2.9 Å from S70OG.

The Ω-loop[28] (residues 161–179) (Fig. 11) forms one edge of the substrate binding side. The two extremities of this peptide stretch are distant by only 3.5 Å. It is an important structural feature of class A β-lactamases which carries the essential residue E166 and contains the short 3_{10} helix H7 (168–170). The conformations of two distorted type II β-turns (173–176) and (177–180) are stabilized by a set of electrostatic interactions consisting of two salt-bridges: R164-D179 and D176-R178. The third residues of each turn (N175 and D179) have strained conformations with respective (Φ, Ψ) values of (67°, 8°) and (61°, 39°). The main chain oxygen atom of residue E177 is not hydrogen bonded to the main chain nitrogen of residue 180 but to T180OG1, a strictly invariant residue. The N and C extensions of the Ω-loop are held together by three hydrogen bonds which involve β-sheet SB (Fig. 12).

The Ω-loop is located at the protein-solvent interface but is strongly linked to the rest of the molecule. Besides one direct hydrogen bond (N170O to E240N), interactions involve 8 buried water molecules and main chain polar atoms of the protein (Fig. 13).

Proper orientation of the catalytic E166 side chain is provided by the *cis* peptide bond formed with P167 and stabilized by a hydrogen bond with N170 side chain and by van der Waals contacts with the buried L169. In addition, its main chain carbonyl and nitrogen atoms are in interaction with the amide group of N136 (Fig. 14).

Four water molecules and a sulphate anion have been identified in the substrate cavity (Fig. 15). They contribute to a complex polar interactions network (Fig. 16) from which only the strong interactions are given in Table IV. The water molecule (WAT297) hydrogen bonded to E166OE1 (2.7 Å) is very likely the one involved in catalysis. WAT323, at 2.8 Å from A237O and N, occupies the oxyanion hole.[29] The sulphate ion is, interestingly, much closer to S130OG (2.9 Å) than to R244 (3.2 Å) which would be accessible for strong salt-bridge interaction. E166OE1 is separated from K73NZ and S70OG by, respectively, 3.4 Å and 4.2 Å. S70OG and S130OG are 3.5 Å apart.

Hydrophobic Clusters and Domains Interface

The contacts between helices H1, H10, and H11 and strands S1, S4, and S5 of the first domain stand on hydrophobic interactions and involve almost all amino acids from one side of those strands. The single polar interaction found within this core arises from Y46: its phenolic group is hydrogen bonded, through the buried WAT369, to one oxygen atom of the solvent shielded side chain of E48. The second

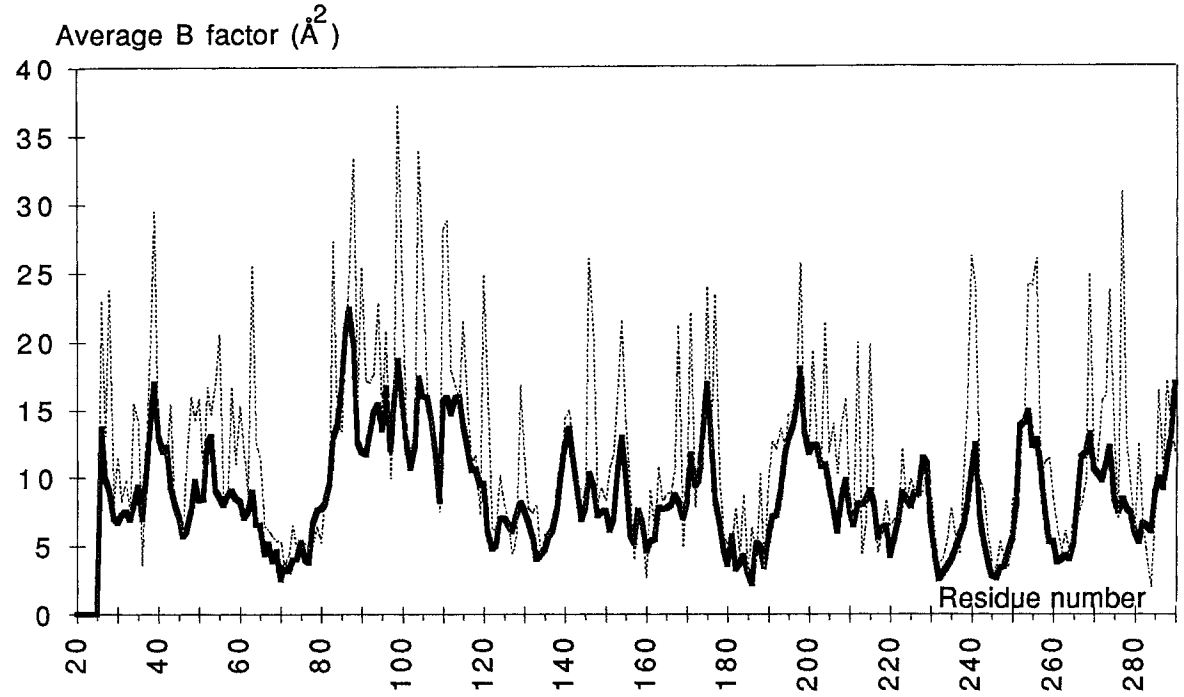

Fig. 3. Average *B*-factors of main chain (thick line) and side chain (dotted line) atoms of TEM1.

oxygen atom of the carboxylate forms a salt-bridge with R259.

The core of the helical domain is also remarkably hydrophobic. Helix H2, the inner element of this domain, contains four polar residues which have a dedicated function: S70, T71, K73, and C77. Helices H2, H8, and H9 are held by an hydrophobic cluster formed by residues V74, G78, and L81 on H2, L190 and L193 on H8, and L207 and M211 on H9. L199 on the connecting loop between H8 and H9 is also pointing toward this interface (Fig. 17). Helix H8 is amphiphilic and each third of its surface, considered along its axis, has a special function: one third is facing H2, one third is solvent oriented, and one third is involved in the two domains interface. Indeed, H8 runs against S1, S4, and S5 providing strong hydrophobic interactions (M186, A187, L190) with residues from those strands (I47, L49, I247, I260, V262). These contacts represent about one half of the whole interface between the two domains. The second half, protected from solvent by the salt-bridge R43-E64, involves residues F66, P67, M69, T71, from the crossover loop, and residues G45, G236, G238, G245, Y264, from S1, S3, S4, and S5 (Fig. 18). In addition, five hydrogen bonds are found. They occur between P67O, WAT321, and T265O, and between Y264OH, T71OG1, M68O, and T71N.

Charge-Charge Interactions and Buried Charged Residues

There are 13 intramolecular and 1 intermolecular salt-bridges in the TEM1 β-lactamase crystal structure (Table V), most of them being located on the protein surface and four of these occurring in the Ω-loop. The aspartate and glutamate residues of salt-bridges E48-R259, R164-D179, and R222-D233 are buried in the protein structure.

Aspartic acids 85, 131, 157, and 214 are also buried. D85, at the C terminus of H2 has its side chain oriented such as to form hydrogen bonds to T200N and S203OG and seems to contribute to the positioning of the N terminus of H9. A special orientation is found for D157 acidic group, whose OD1 is hydrogen bonded to T160OG1, which is itself hydrogen bonded to T181OG1. This buried aspartic acid side chain seems to determine the proper orientation of the 2 threonine side chains in order to orient T181CG2 in the hydrophobic interface between the two protein domains, at van der Waals distance of Y264 aromatic ring. The role of D131 in the topology of the substrate cavity has already been described. D214 belongs to the peptide stretch forming the second hinge region. Its carboxylic group is hydrogen bonded to D233OD1 and to the buried WAT309 of the active site (Figs. 9, 16).

Solvent Structure

A total of 199 water molecules, as well as a sulphate anion in the active site, have been identified in the structure of β-lactamase TEM1. The average occupancy and the average temperature factor of water molecules are 0.61 and 15.1 Å^2, respectively. There is a layer of water molecules at the contact

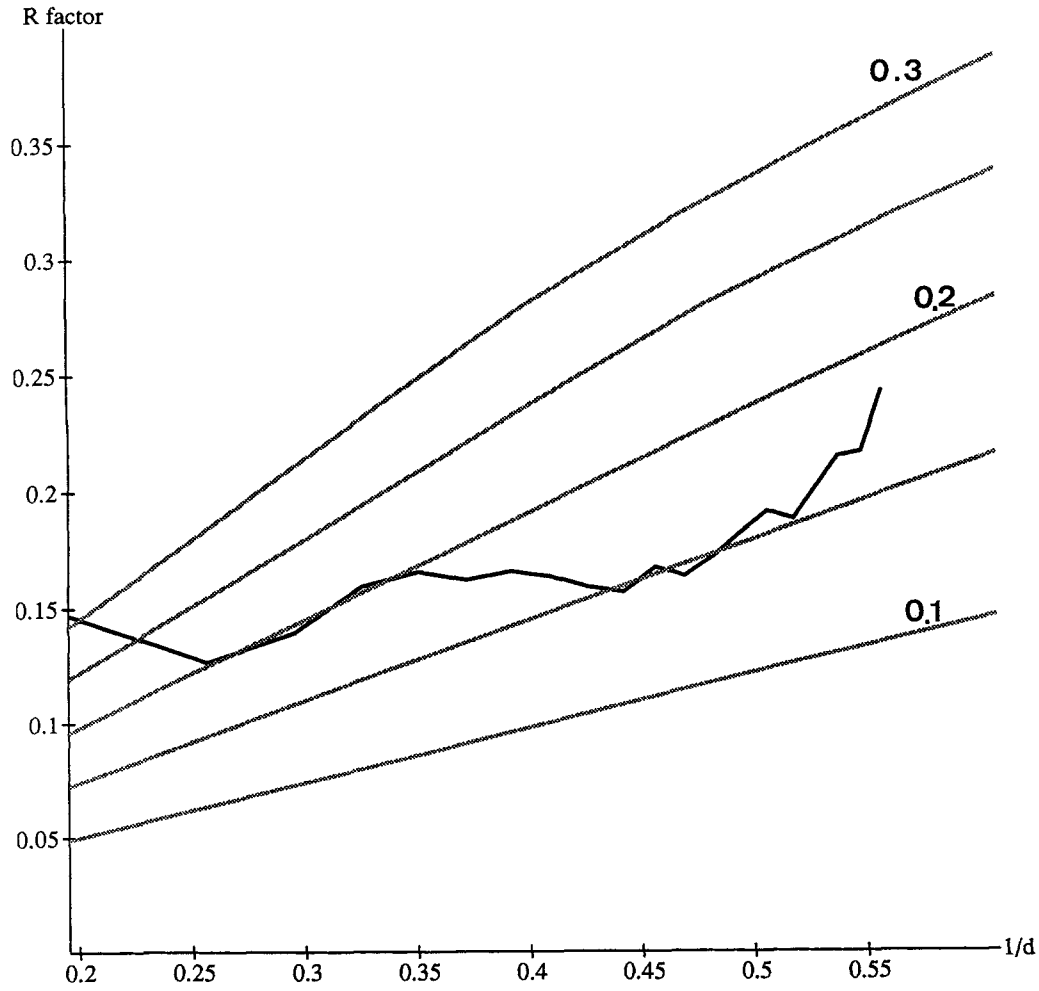

Fig. 4. Evolution of the crystallographic *R*-factor as a function of the inverse of the resolution, superimposed on theoretical *R*-factors deduced from mean coordinate errors.[23]

areas of symmetry-related protein molecules. It represents, together with van der Waals contacts, the major crystal packing interactions. Indeed, there are only a dozen direct hydrogen bonds and one salt-bridge between atoms of symmetry-related molecules.

DISCUSSION

The structure of the TEM1 enzyme was solved by multiple isomorphous replacement, although molecular replacement using the PC1 structure provided the right solution. The low rotation and translation functions signals are likely related to the different domain-domain orientations that are described in details in a later paragraph.

The general fold of the TEM1 enzyme is similar to the one found in previously determined class A β-lactamase structures. The protein is formed of two domains, connected by two hinge regions, and displays remarkable long-range polar interaction networks whose analysis is relevant with respect to the following points: conformational change during catalysis, response to mutations leading to extended substrate specificity within the TEM family, and different catalytic efficiencies within class A enzymes.

Class A β-lactamases from different sources exhibit different substrate specificities but all essential residues, except R244, implicated in catalysis, are conserved. The TEM1 enzyme is peculiar, as it generates by point mutations a set of naturally occuring proteins with extended substrate specificities.[2] It thus seems that this enzyme is an excellent candidate to possibly unravel the molecular mechanism by which a protein could exhibit full enzyme efficiency[30] while changing substrate specificity. This goal should be achieved by accurate kinetic measurements on TEM1 enzyme and site-directed mutants of the protein, with a given set of enzyme substrates, coupled with X-ray structure determinations.

The amount of solution data on class A β-lactamases and on their site-directed mutants is quite

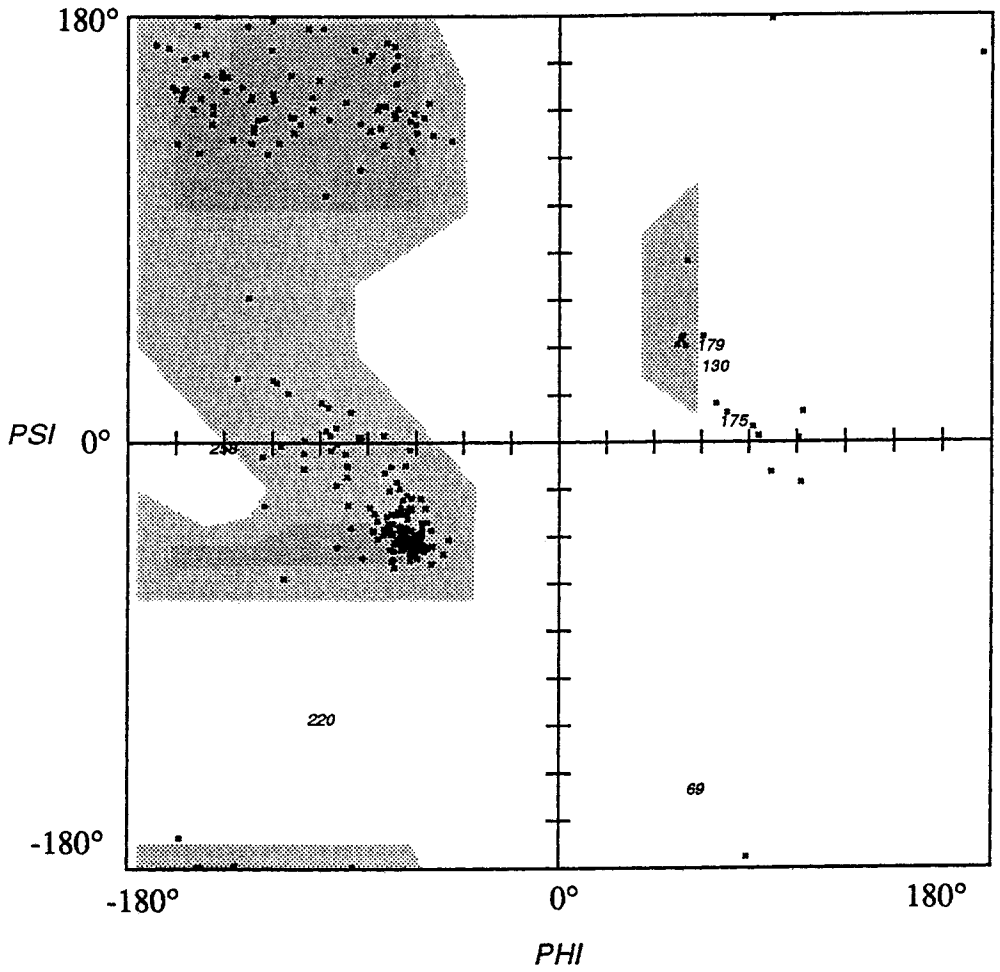

Fig. 5. Ramachandran plot of TEM1. Non-glycine residues in unfavorable conformations are labeled.

significant. However, it sometimes turns out that data on enzymes from different sources are merged with the aim of providing a consensus view of some properties. Such approach, which assumes structural identities between those enzymes and anticipates the conformational effects of amino acid substitution, may lead to a confusing picture. The analysis and discussion of the TEM1 structure will, thus, often refer to the available *S. aureus* PC1 crystallographic structure (Protein Data Bank entry: 3BLM), sequence alignments within the class A family, and exclusively, to site-directed TEM1 mutants.

The Central Helix H2

H2 is one helix turn longer in TEM1 compared to PC1. D85, a specific residue of Gram$^-$ enzymes, is located in this turn and there is no equivalence in PC1 of its interaction with S203OG. This helix does not have the same sequence in both β-lactamases. This is especially reflected in the polarity of the cavity found in the vicinity of E166. In TEM1, this area is quite hydrophobic and contains F72, L76, A135, L139, P145, L148, and L162 whose side chains display optimal van der Waals interactions (Fig. 19). In PC1, the replacement on F72 and L162 by, respectively, serine and proline, empties the cavity which is filled by the side chains of residues N76 and N135. It results in a totaly different character of the cavity in which water molecules have been located.[8]

T71 was shown to be essential to proper structural stability of TEM1.[31] The side chain of threonine 71 extends from helix H2 toward the domains interface of the protein. The hydroxyl group forms two important hydrogen bonds with the hydroxyl group of Y264 and with M68 main chain oxygen atom, while T71CG2 is at about 4.5 Å from residues 235–236 main chain atoms.

The disulfide bridge (C77-C123) connects helices H2 and H4 and is found in 7 out of 20 class A β-lactamases.[5] Removal of this covalent link by site-directed mutagenesis (C77S) led to an enzyme with the same activity but reduced thermostability at

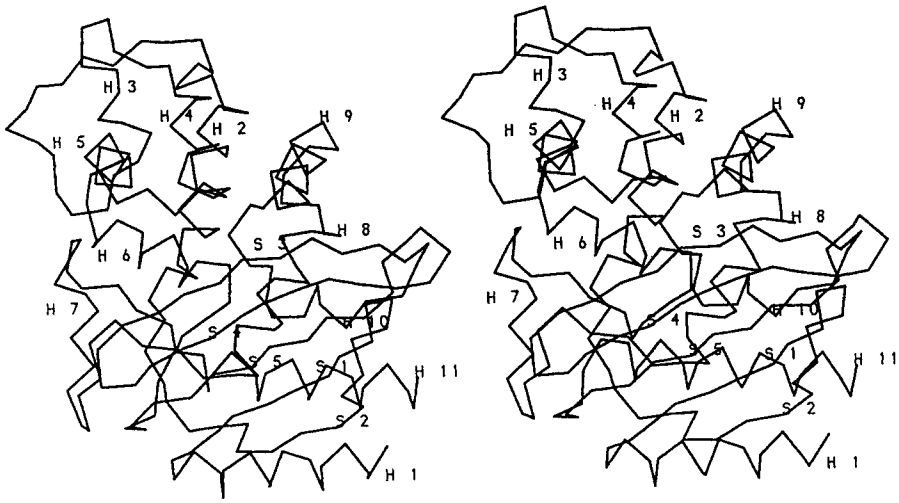

Fig. 6. Stereo view of the Cα-backbone of TEM1 β-lactamase. The secondary structure elements are labeled according to Table III.

TABLE III. Secondary Structural Elements in TEM1 β-Lactamase*

Helices			Antiparallel β-sheets	
H1	α	26–40	Main β-sheet	
H2	3_{10}	69–71	S1	43–50
	α	72–85	S2	56–60
H3	3_{10}	109–111	S3	230–237
H4	α	119–128	S4	244–251
H5	α	132–142	S5	259–266
H6	α	145–154	Sheet B	
H7	3_{10}	168–170	SB1	66–67
H8	α	183–195	SB2	180–181
H9	α	201–212	Sheet C	
H10	3_{10}	221–224	SC1	94–95
H11	α	272–288	SC2	117–118
Disulfide bridge	Cys 77-Cys 123			
β-bulge	57, 58, 48			

*Residue numbering according to Ambler et al.[5]

40°C, while the enzyme is unstable upon mutations of both C77 and T71.[32]

Hinge Regions and Domains Interface

The two hinge regions are held by charge-charge interactions. Two glutamic acids (37 and 64) and two arginine residues (43 and 61), which are not all strictly conserved within β-lactamases, are involved in the first one. In the PC1 enzyme, the R43H, R61N, and E64K mutations lead to much weaker interactions between domains. The salt-bridge between residues R222 and D233 determines the conformation of the second hinge region and explains the strained (−103°, −117°) dihedral angles of L220. Consistently, replacement of D233 in TEM1 by other amino acids reduces strongly the catalytic activity.[33]

In *Klebsiella pneumoniae*, PIT-2, *Pseudomonas aeruginosa*, and TEM β-lactamases, position 214 is occupied by an aspartic acid. In the TEM1 structure, the buried D214 has its side chain hydrogen bonded to one of the carboxylic oxygens of D233 and to water molecule 309 which interacts with K234 in the active site (Fig. 16). Such proximity of aspartic residues should increase the pKa of one of the acidic groups. D233, which forms a salt-bridge with R222, is invariant whereas D214 is only found in 4 out of 20 class A β-lactamases. As the overall conformations in this area are quite similar in TEM1 and PC1 enzymes, where an asparagine is found at position 214, it is likely that the protonated residue is D214.

At the interface between domains, G45 is facing P183 and F66. These residues are strictly conserved and no other residue than G45 could be sterically accomodated. In contrast to *B. licheniformis* β-lac-

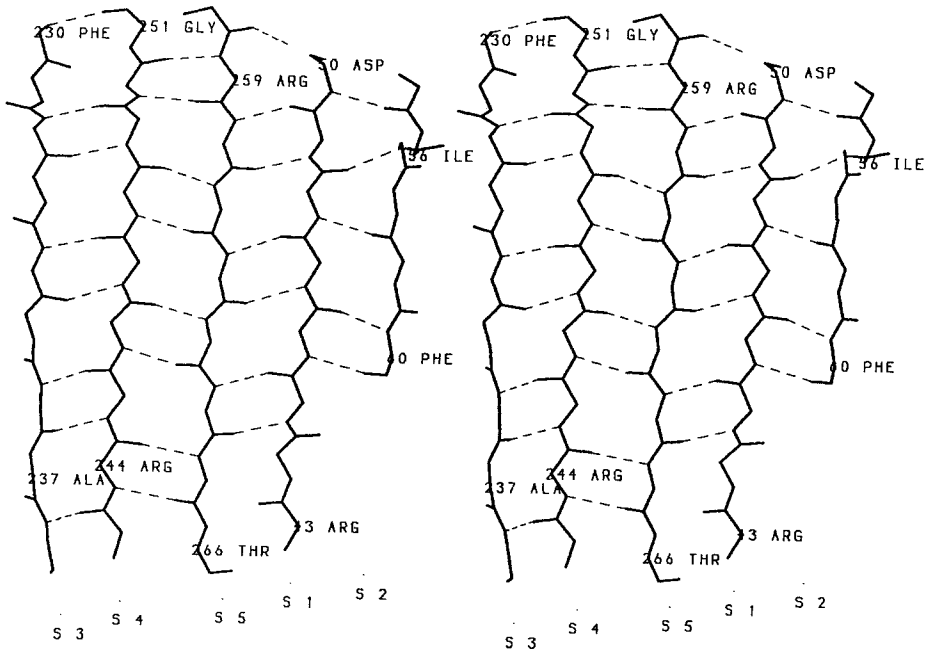

Fig. 7. Stereo view of the main chain atoms of the five-stranded antiparallel sheet. Hydrogen bonds are indicated by hatched lines.

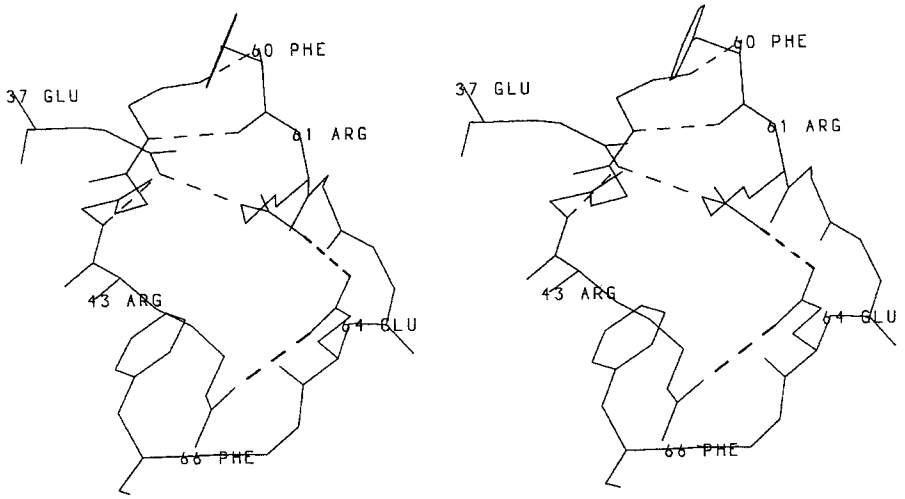

Fig. 8. Hydrogen bonds and charge-charge interactions (hatched lines) at the first hinge region.

tamase structure,[9] there is no water molecule buried in this area. G245 is replaced by N245 in PC1. This significant increase in sterical volume, in such an important area, is compensated by the M69A mutation which creates a small cavity which is filled by the methyl group of A238. In this position, a glycine residue is almost always found in β-lactamases. Residue 69 is quite variable in size and character among class A enzymes but is always found in a high conformational energy.[8,9] Although it seems that its mutation could be accomodated without major rearrangement in the TEM1 structure, the M69L mutant displays marginally perturbed kinetic behavior but shows dramatically decreased irreversible inactivation by both clavulanic acid and sulbactam.[34]

The D157-T160-T181 interaction found in TEM1 seems to provide the proper orientation of T181CG2 toward Y264 aromatic ring. A similar hydrogen bonds pattern is found in PC1 but the mutation T181S creates a cavity delineated by residues F66, P183, F186, and F264. F66 and P183 are conserved between the two enzymes, but small movements of

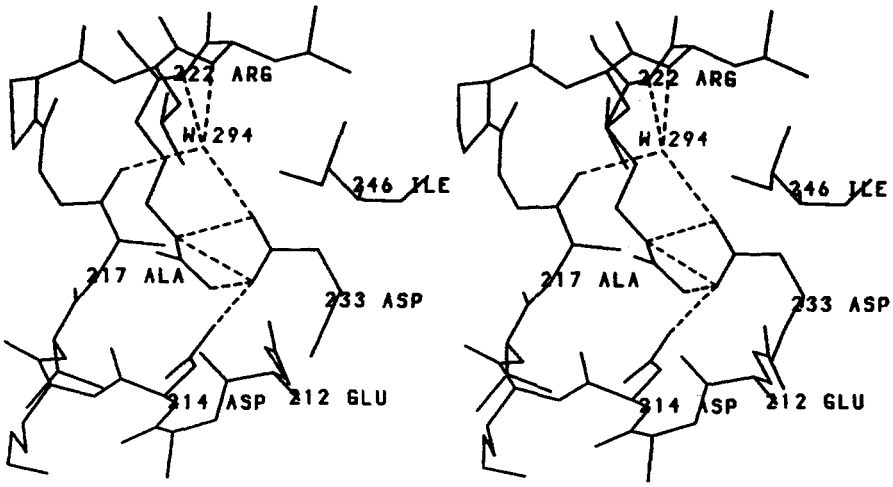

Fig. 9. Stereo view of the second hinge region showing hydrogen bonds and charge-charge interactions (hatched lines): D214 and D233 are buried. WAT294 stabilizes the conformation of the loop 217–222.

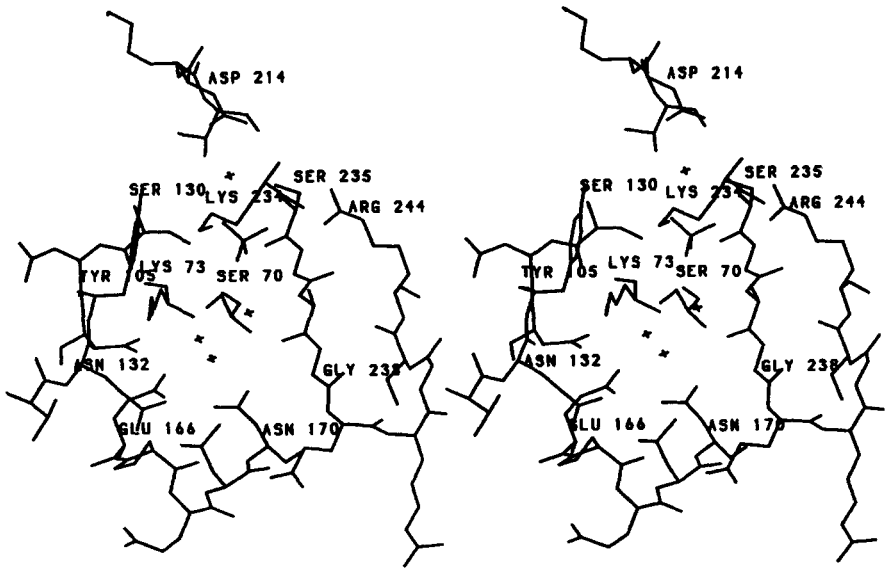

Fig. 10. Stereo view of the substrate binding cavity.

their side chains and the important mutation M186F in PC1, compensate for the T181S substitution. The mutation Y264F, however, results in the loss of the hydrogen bond with T71OG1, which, as earlier mentioned, seems important for TEM1 stability.

The Substrate Binding Site

P107 is a strictly conserved residue in class A β-lactamases. In TEM1 it appears as the second residue of a distorted type I turn. The conformation of this motive is strongly influenced by the hydrogen bond between T109N and the acidic group of the invariant and buried D131 which also requires, as hydrogen bond partner, a hydroxyl group on the side chain of the fourth residue of this turn. This explains that serine or threonine are always, except twice, found at position 109.

Residue 167 is a proline in 13 out of the 20 class A β-lactamases. However, a *cis* peptide bond has also been observed between E166 and I167 in PC1 crystal structure, which emphasizes its role for a proper location and orientation of E166.

Strand S3 forms one side of the substrate binding cavity and bears residues which are important for enzyme stability or activity. S235 is a potential hydrogen bond partner and was shown to interact with the carboxylate of PenG.[11] Any other residue than

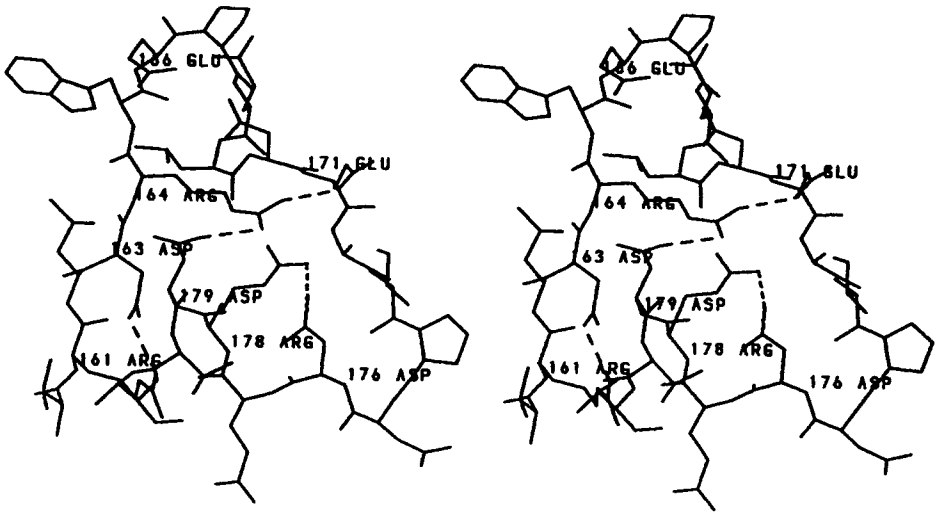

Fig. 11. Stereo view of the Ω-loop and of the four salt-bridges of TEM1 enzyme.

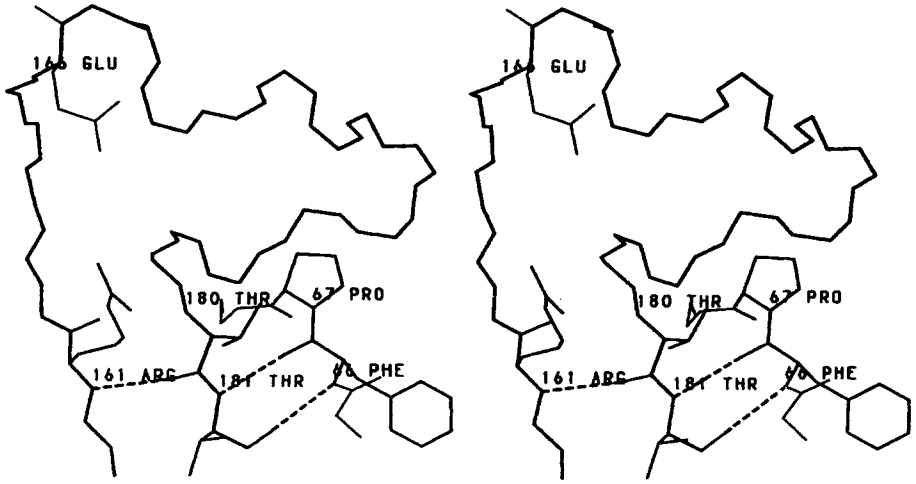

Fig. 12. Stereo view of the N and C termini of the Ω-loop. Residues 66–67 and 180–181 form sheet B.

G236 would have its side chain directed toward M69CB, main chain atoms of residues 70–71 and T71CG2, which might explain its invariance in β-lactamases. It has, nevertheless, been observed that phenotypes containing G236 TEM1 mutants can resist to ampicillin at very low concentrations of the antibiotic.[33]

A237CB is pointing toward the substrate binding site, at 4 Å distance between M272 and R244 side chains, and should provide the main steric constraint for the substrate position on this side of the cavity. Residue 237 is usually an alanine or a glycine in other class A β-lactamases. Bulkier amino acids are, however, also found at that position and a threonine residue is even found in TEM5 natural mutant. Its side chain could either be oriented toward the substrate binding site, impairing binding, or partially oriented toward R244, M272, and R275 generating steric conflicts that can only be released through displacement of some residues. In any case, substrate binding and/or local structure should be affected. Interestingly, the A237N TEM1 mutant displays a lower kcat toward penam substrates but a higher activity with cephem antibiotics.[35]

The significant mutation A237Q occurs in the PC1 enzyme. This residue cannot be simply accomodated in the TEM1 structure because Q237 and M272 side chains would collide. This observation points to the important fact that the region 265–276 is quite different in these enzymes, with respect to sequences, conformations, and locations. Those differences have many consequences and arise because helix H11 is one turn longer in TEM1 (residues 272–274) than in PC1. As a consequence, P274 in PC1 is

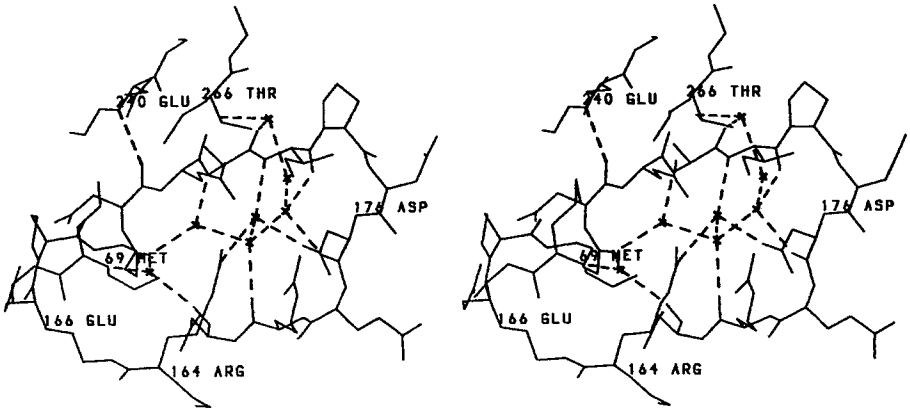

Fig. 13. Buried water molecules involved in the interactions between the Ω-loop and the protein core.

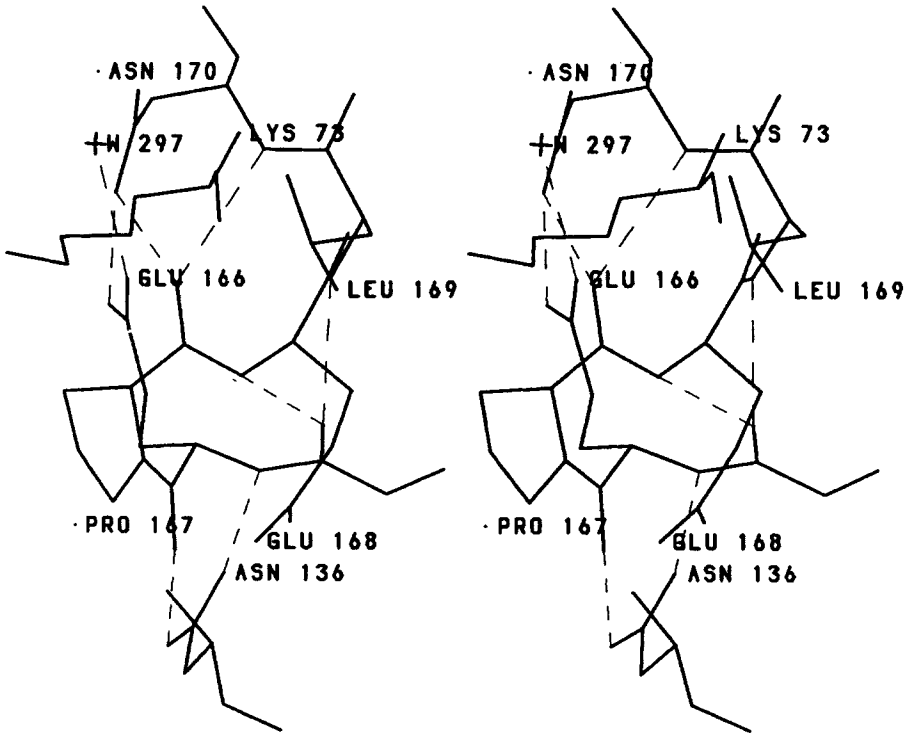

Fig. 14. Stereo view of the *cis* peptide bond 166–167 and of the surrounding hydrogen bonds (hatched lines) that maintain the conformation of E166.

found at the same spatial location as the R275 side chain in TEM1, a residue only found in Gram$^-$ enzymes, and the distance between CA atoms of residues 271 from the two proteins amounts to 9 Å. These observations prompted us to analyze the sequences of β-lactamases of known three-dimensional structures at positions 246, 220, 244, and 276, taken in this order to illustrate the pairwise spatial proximities.

In TEM1 (I246, L220, R244, N276), R244 side chain has restricted movements as it is hydrogen bonded to N276 and at van der Waals distances of L220, A237, and M272 side chains. Residue 246 is buried and at van der Waals distance of residue 220.

In PC1 (D246, L220, R244, and D276) the availability of the positive charge of R244, implicated in the enzyme mechanism, should be reduced by the salt-bridge R244-D276 as in the *B. licheniformis* β-lactamase (Protein Data Bank entry: 4BLM). Those two enzymes are identical with respect to the conformation of residues 265–276 and to the amino acids occurence at all four positions mentioned

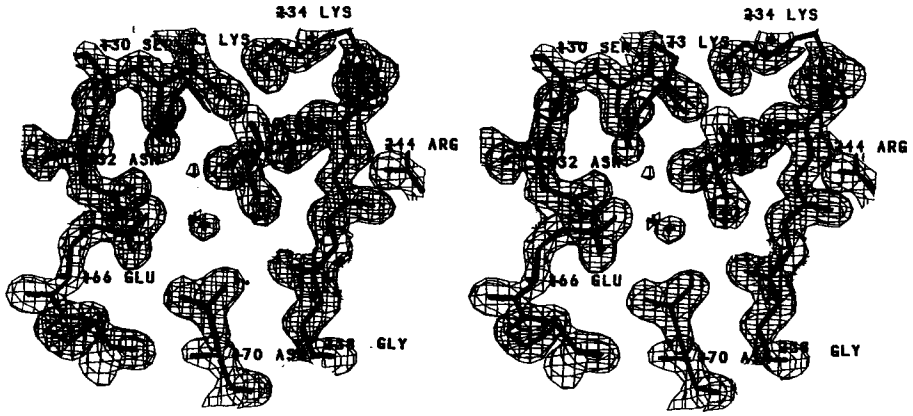

Fig. 15. Electron density map ($2F_{obs} - F_{calc}$, Φ_{calc}) of the catalytic region. The contour level is 1.0 σ. Crosses indicate the water molecules.

above. The expected decrease in electrostatic potential normally produced by R244 is consistent with the fact that the cacodylate ion, found in the *B. licheniformis* β-lactamase crystal structure, is at hydrogen bond distance from S130G and S70G but at 5.9 Å from the R244 guanidinium group. In *S. albus* G (D246, R220, N244, D276), R220 has been postulated to replace R244 function.[36] Nevertheless, the buried D246 in the vicinity of R220, and the presence of D276, may reduce the effective positive charge of the guanidinium group. It is only in *B. cereus* 569[37] (D246, L220, R244, N276) and in *E. coli* TEM1 β-lactamases that R244 has no negative charge in its neighborhood.

G238, as already mentioned, is imposed by the presence of M69 side chain and N170. Its mutation to serine, however, occurs in TEM3 and TEM4 β-lactamases. The minimum displacement possible to accomodate this side chain would be to move N170 which belongs to the Ω loop.

The insertion of residue I239 occuring in PC1, in the turn between β-strands S3 and S4 (238–243), also creates local differences between PC1 and TEM1 β-lactamases at this edge of the catalytic cleft. The conformations of the loops in both enzymes are different.[10] As a consequence, the important main chain atoms of residue 237, whose nitrogen atom is part of the oxyanion hole, occupy slightly different positions in PC1 and TEM1 enzymes.

Stability and Conformational Aspects of the Ω-Loop

Part 171–173 of the Ω loop is in close vicinity to regions 66–67 and 238–241 of the protein. The crossover loop (60–68) has identical conformations in the two enzymes, although the sequences display significant differences. From TEM1 to PC1 enzymes, the following mutations are observed: P67A, E171Y, A172Y, I173S, and G238A, E240T, R241Y. They change the marked polar character of this region in TEM1 to a rather hydrophobic one in PC1. This could be related to the evolutionary capacity of the TEM1 enzyme because mutations at some of these positions are responsible for altered substrate specificity.

A172 is in α_L conformation and the four next residues (I, P, N, D) form a distorded type II β-turn. The (Φ, Ψ) dihedral angles of N175 are strained in order to release the steric conflict between its CB atom and P174 main chain oxygen atom. Actually, in most β-lactamases sequences, a glycine residue is found at position 175.

The salt-bridge R164-D179 is strictly conserved among class A β-lactamases, and links the two ends of the Ω-loop. The P54 mutant D179N of the β-lactamase PC1 has a drastically reduced catalytic activity. A crystallographic study of this PC1 mutant[11] showed that removal of this link leads to a substantially disordered Ω-loop. It should, however, be mentioned that among the four salt-bridges of the Ω-loop observed in TEM1, only one (R164-D179) remains in the PC1 β-lactamase. The Ω-loop in the TEM enzyme is thus much more constrained.

Catalytic Residues

Except for R244, all residues involved in catalysis are invariant among class A β-lactamases. S70, K73, S130, E166, and K234 have clear electron density (Fig. 15) and refined to low temperature factors in the TEM1 structure. Together with water molecules and a sulphate ion, they are involved in complex hydrogen bond interactions (Fig. 16). The analysis of these interactions needs care because hydrogen bond distances range from 2.7 to 3.3 Å and their description as strong, medium, or weak, especially with respect to their significance in the catalytic mechanism, should also take into account the side chain mobilities. The flexibility of K73 side chain, located between S70 and E166, is large and tenths of an angstrom are easily gained or lost upon

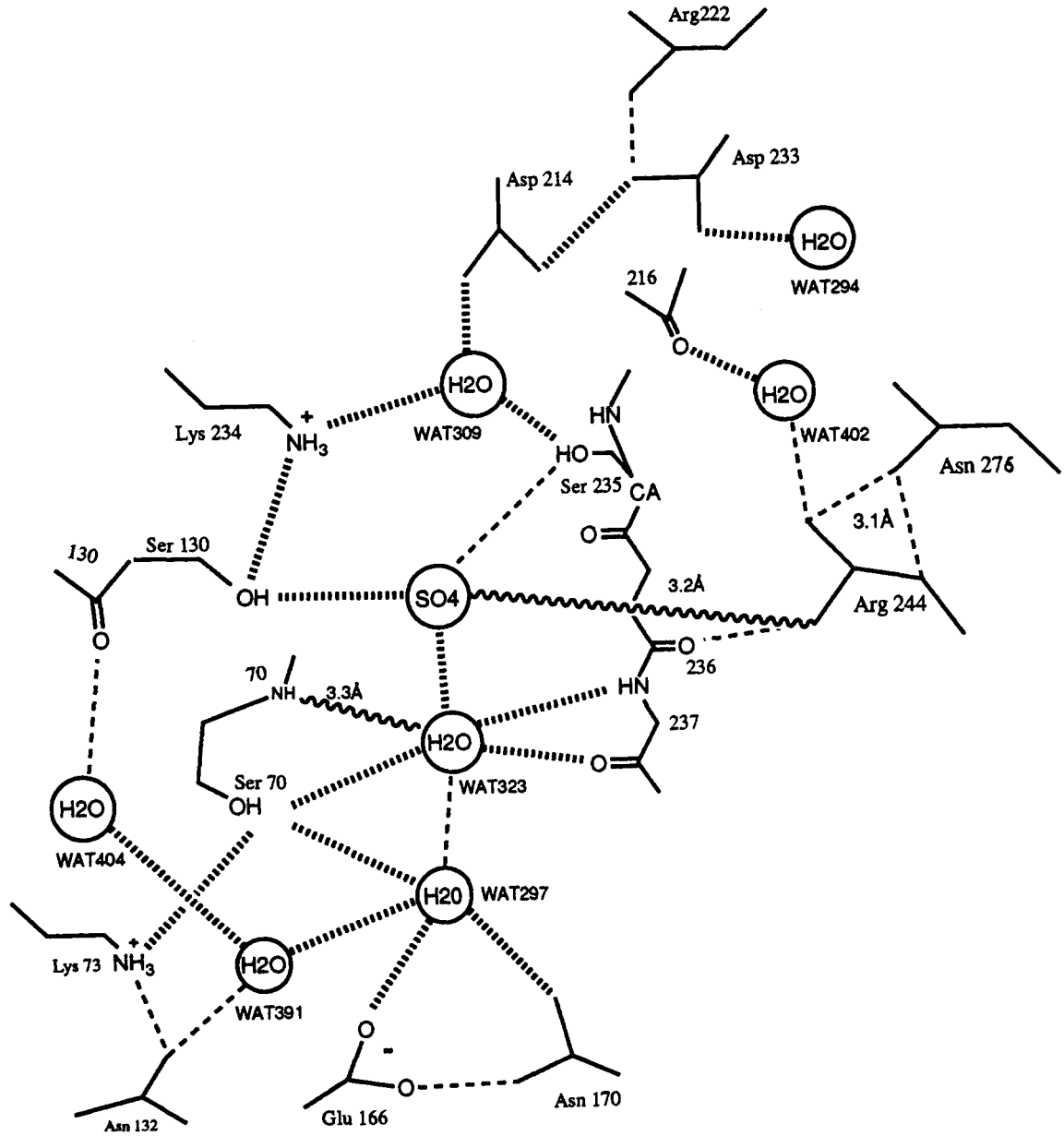

Fig. 16. The interactions network in the catalytic site. Hatched lines indicate hydrogen bond distances less than 2.9 Å. Dotted lines are used when the distance is above that value. Wavy lines are for special cases (see text).

variation of the χ1 dihedral angle of S70 and S130. For instance, the distance between K73 and S130 side chains was reported to be 3.7 Å in the TEM1 structure and 2.8 Å in the acylated complex.[11] In our refined TEM1 structure, the S130OG-K73NZ distance is 4.2 Å whereas it amounts 3.2 Å and 3.7 Å in *B. lichenformis* and *S. aureus* β-lactamases, respectively. This difference, illustrative of the already mentioned flexibility of the K73 side chain, might be a consequence of the electrostatic effect produced by the sulphate ion, found at 2.9 Å from S130OG and at 3.2 Å from the accessible guanidinium group of R244.

According to the closest proximities observed, the active site could, tentatively, be divided into two areas. There are consecutive hydrogen bonds between, on one hand, the sulphate ion, S130, K234, WAT309, D214, D233, and R222 (WAT309 is also at 2.9 Å from S235OG) and on the other hand, K73, S70, WAT297, and E166 (Fig. 16). These two networks are connected through the WAT297-WAT323 sulphate ion interactions. WAT297, between S70

TABLE IV. Major Interactions Within the Active Site of the Enzyme

Interactions		Distances (Å)
S70OG	K73NZ	2.9
S70OG	WAT323	2.9
S70OG	WAT297	2.9
E166OE1	WAT297	2.7
E166OE2	N170ND2	3.0
N170OD1	WAT297	2.8
A237O	WAT323	2.8
A237N	WAT323	2.8
S130OG	SO4	2.9
R244NH1	SO4	3.2
K234NZ	S130OG	2.9
K234NZ	WAT309	2.9
S235OG	WAT309	2.9
D214OD1	WAT309	2.9
WAT297	WAT391	2.8
WAT323	SO4	2.8

TABLE V. Salt-Bridges in TEM1 β-Lactamase*

Salt-bridge		Distance (Å)
Lys32	Asp35	3.0
Lys34	Asp38	3.1
Glu37	Arg61	2.9
Arg43	Glu64	2.9
Glu48	Arg259	2.8
Arg61	Glu64	3.0
Lys73	**Glu166**	3.4
Glu89	Arg93	3.1
Arg161	Asp163	2.9
Arg164	Glu171	2.7
Arg164	**Asp179**	3.0
Asp176	Arg178	3.0
Arg222	**Asp233**	3.1
Intermolecular crystal contacts		
Lys32	Glu197	3.0

*Invariant residues are in bold type.

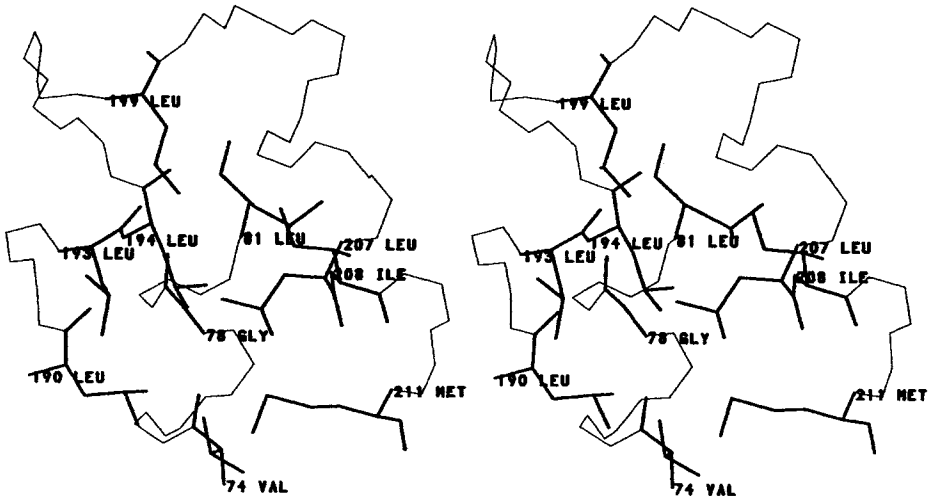

Fig. 17. Hydrophobic core between H2, H8, and H9. N-Cα-C backbone, thin lines; side chain atoms of residues involved in non-polar interactions, thick lines.

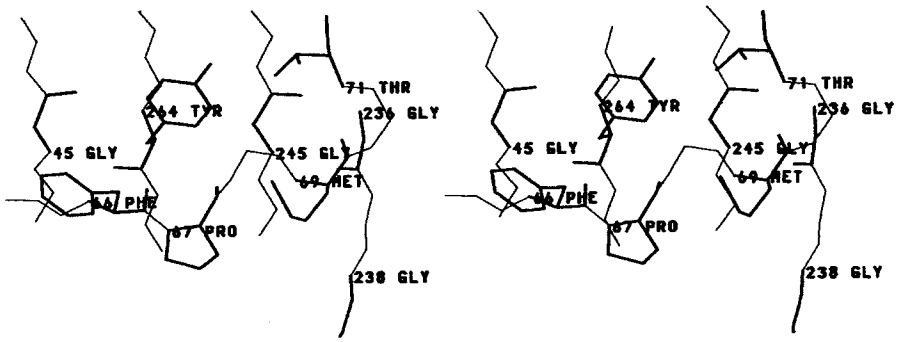

Fig. 18. Hydrophobic interactions at the interface of the two protein domains which involve the polypeptide stretch 66–71 (N-Cα-C backbone).

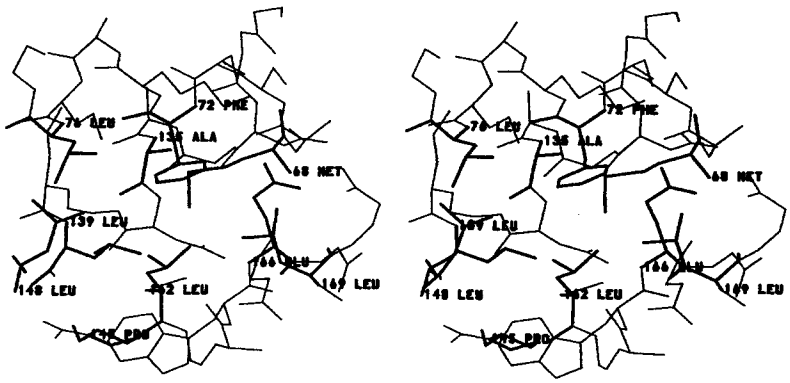

Fig. 19. The hydrophobic cavity in the vicinity of the residue E166 of TEM1 enzyme.

and E166, is in proper position as partner of the deacylation step and WAT323, 2.8 Å from A237 main chain atoms and 3.3 Å from S70N, occupies the oxyanion hole.

A number of active site mutants of TEM1 have been studied. E166 mutant enzymes properties[38,39] demonstrated the role of this glutamic acid in the deacylation step, and similar conclusions were drawn from the X-ray study of the E166A mutant of *B. licheniformis* β-lactamase.[12] Acylation by S70 on the *ré* face of the β-lactam ring was shown in the crystal structure complex of the E166N mutant with PenG.[11] It was then proposed that in the enzyme mechanism, K73NZ, located at 3.4 Å from E166OE1, acts as a general base in the acylation step.

K234 is non-accessible to bulk water and the importance of the positive charge of its side chain, found at 2.9 Å from S130OG, has been analyzed by site-directed mutagenesis in K234R and K234T TEM1 mutants.[40] The drastic opposite kinetic effects resulting from these mutations led to the conclusion that K234 is involved in substrate binding and transition state stabilization. The evaluated contribution of the K234 side chain to apparent binding energy in the transition state is 4.6 kcal/mole. The R244Q or T and R244K or S mutants of TEM1 have been produced and studied.[34,41] Kinetic results from these independent investigations show that kcat values for PenG substrate are nearly unaffected by the nature of the residue at position 244, the apparent binding energy of R244 side chain to the transition state being around 2 Kcal/mole. These data, obtained in solution with site-directed mutants of the TEM1 enzyme would support a stronger interaction of the carboxylate group at C-3 of the substrate with K234 than with R244 in the transition state, whereas the interaction with R244 would dominate after acylation.[11]

Superposition of TEM1 and PC1 Crystal Structures

The Cα coordinates of β-lactamases PC1 and TEM1 have been superposed by least-squares fitting, after omission of the largest differences (residues 26–30, 50–58, 84–91, 238–242, 250–258, and 265–275). The root-mean-square deviation for the corresponding Cα atoms is 1.86 Å (without omission: r.m.s. = 2.49 Å). This is to be compared to the lower r.m.s. deviation of 1.37 Å found between PC1 and *B. licheniformis* enzymes.[42]

Inspection of the superimposed structures showed that rigid body handling of the whole protein structures was not satisfactory. Indeed, the two enzymes are best superimposed when their two domains are handled independently and rotated in opposite directions along nearly parallel axes running through each domain (Fig. 20). Overall, these rotations amount to 7° and result in a wider opening of the substrate cavity in PC1 compared to TEM1. The catalytic properties and the substrate specificities of the TEM1 and PC1 enzymes are probably influenced by this different aperture of the substrate binding cleft as well as by the many local structural and sequence differences already pointed out.

Mutated Residues in Extended Spectrum TEM β-Lactamases

The TEM1 β-lactamase hydrolyzes penicillins and some first and second-generation cephalosporins. One to four point mutations can extend the hydrolysis spectrum of the TEM β-lactamase to some third-generation cephalosporins, especially ceftazidime and cefotaxime.[1–3] The location of the mutated residues in the TEM1 structure is displayed in Figure 21.

The extended spectrum TEM β-lactamases derive from TEM1 or TEM2, two enzymes with identical enzymatic properties and only differing by the Q39K mutation. Residue Q39 is located at the C terminus

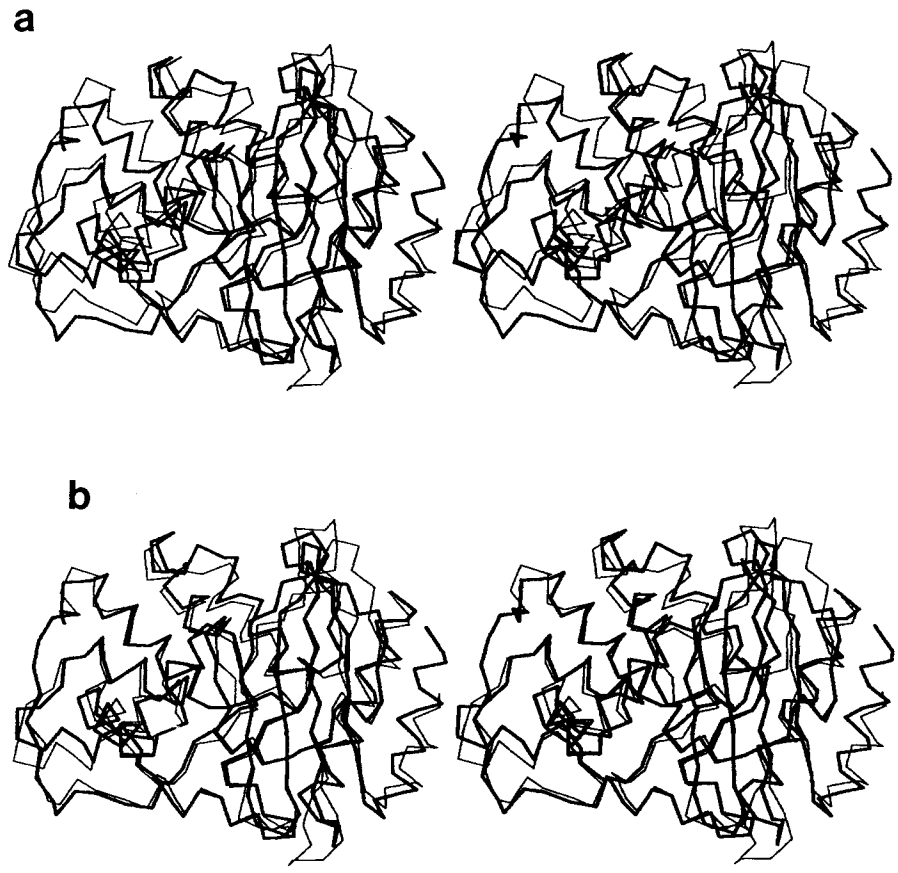

Fig. 20. Superposition of TEM1 (thick line) and PC1 (thin line) β-lactamases. **a:** Cα atoms of the β-domains (except loops and INDEL regions) from both proteins were superimposed by least-square procedures and the resulting transformation matrix applied to all Cα atoms. **b:** Cα atoms from each domain (except loops and INDEL regions) were handled independently.

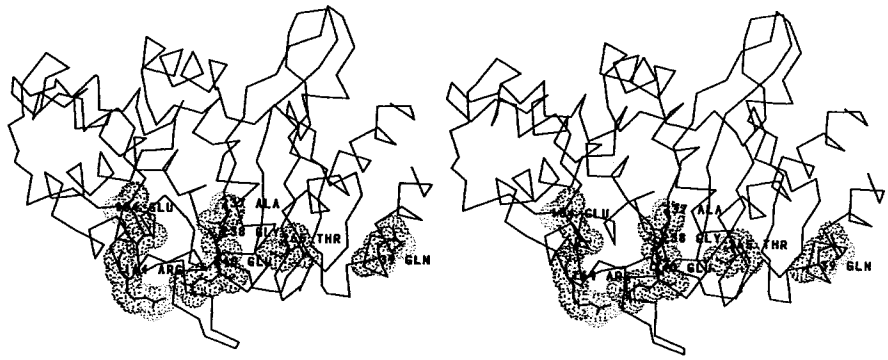

Fig. 21. Stereo view of the Cα-backbone of TEM1 enzyme and van der Waal surfaces of the residues that confer, upon mutation of the TEM enzyme, extended substrate specificities.

of helix H1 at the protein-solvent interface, far from the active site. Its side chain amide group interacts with D35 carboxylic acid through 2 water molecules. Additionally, D35 forms a salt-bridge with K32 which also interacts with Q278 from H11. The E104K, R164S, and G238S mutations are found in natural protein mutants which derive from TEM1 or TEM2 enzymes. The X-ray structure of TEM1 does not provide an explanation of whether Q or K at position 39 might favor the occurence of further mutations.

E104 and E240 are at the protein-solvent interface, at the entrance of the substrate binding cavity, and their side chains are not involved in specific

interactions. However, E104, in the neighborhood of P167, could interact with the C-6 side chain of penam substrates, and its substitution to a lysine would affect the kinetic properties of the resulting mutant. E240 is part of the tight loop connecting S3 and S4. Further crystallographic investigations seem necessary in order to explain the higher catalytic efficiency of the E240K mutant enzyme toward cephalosporines compared to the wild type protein.[3] However, the proximity of E171 and E168 should be mentioned because interactions between K240 and those residues would affect the conformation of the Ω loop.

Two of the four charge-charge interactions that stabilize the Ω loop in TEM1 are formed between R164 and D179, E171. Their disruption upon R164S or H mutation will certainly destabilize this region but the redistribution of charges cannot be anticipated.

R244 and T265 are adjacent residues on strands S4 and S5. One buried water molecule bridges T265OG1 to G242O and S268N. T265CG2 is oriented toward R244 side chain. The mutation T265M would disrupt this buried hydrogen bond pattern and might lead to structural modifications in this region.

CONCLUSIONS

The molecular structure of the TEM1 enzyme allows the first comparison of Gram$^-$ and Gram$^+$ β-lactamases. This analysis gives some insights into the structural reasons that may account for the different kinetic properties, substrate specificities, and evolutionary capabilities encountered for TEM1 compared to the PC1 enzyme. The TEM1 wild-type structure cannot provide definite explanations about the structural events occuring upon the mutations which lead from TEM1 or 2 to TEM3–TEM15 enzymes[43] and further crystallographic studies are required. The density of strong interactions throughout the molecule would seem prohibitive to large conformational changes but, on the other hand, some of them could easily be reshuffled in order to accomodate local movements. The area, interestingly defined by loops 103–106, 238–241, 266–275, and Ω, deserves special attention. There are, in many respects, differences between TEM1 and PC1 enzymes which impair the structural explanations on TEM1 mutants based on the PC1 enzyme structure and the generalization of the conclusions drawn from one enzyme to the other. The X-ray coordinates of the TEM1 enzyme will be deposited in the Brookhaven Data Bank.

ACKNOWLEDGMENTS

We thank Dr. Dino Moras and collaborators at the UPR de Biologie Structurale in Strasbourg for all facilities placed at our disposal throughout this work. C.J. was employed during his Ph.D. by Biostructure SA, Les Algorithmes, Parc d'Innovation, 67400 Illkirch-Graffenstaden, France. This research was funded, in part, by the French Ministry of Research and Technology (Grant 89T0840).

REFERENCES

1. Phillippon, A., Labia, R., Jacoby, G. Extended-spectrum β-lactamases. Antimicrob. Agents Chemother. 33:1131–1136, 1989.
2. Collatz, E., Tran Van Nhieu, G., Billot-Klein, D., Williamson, R., Gutmann, L. Substitution of serine for arginine in position 162 of TEM-type β-lactamases extends the substrate profile of mutants enzymes, TEM-7 and TEM-101, to ceftazidime and aztreonam. Gene 78:349–354, 1989.
3. Sowek, J.A., Singer, S.B., Ohringer, S., Malley, M.F., Dougherty, T.J., Gougoutas, J.Z., Bush, K. Substitution of Lysine at position 104 or 240 of $TEM1_{pTZ18R}$ β-lactamase enhances the effect of serine 164 substitution on hydrolysis or affinity for cephalosporins and the monobactam aztreonam. Biochemistry 30:3179–3188, 1991.
4. Joris, B., Ghuysen, J.M., Dive, G., Renard, A., Dideberg, O., Charlier, P., Frère, J.M., Kelly, J.A., Boyington, J.C., Moews, P.C., Knox, J.R. The active-site serine penicillin-recognizing enzymes as members of the *Streptomyces* R61 DD-Peptidase family. Biochem. J. 250:313–324, 1988.
5. Ambler, R.P., Coulson, A.F.W., Frère, J.M., Ghuysen, J.M., Joris, B., Forsman, M., Levesque, R.C., Tiraby, G., Waley, S.G. A standard numbering scheme for the class A β-lactamases. Biochem. J. 276:269–272, 1991.
6. Bush, K. Classification of β-lactamases: Groups 1, 2a, 2b and 2b′. Antimicrob. Agents Chemother. 33:264–271, 1989.
7. Dideberg, O., Charlier, P., Wéry, J.P., Dehottay, P., Dusart, J., Erpicum, T., Frère, J.M. Ghuysen, J.M. The crystal structure of the β-lactamase of *Streptomyces albus* G at 0.3 nm resolution. Biochem. J. 245:911–913, 1987.
8. Herzberg, O. Refined crystal structure of β-lactamase from *Staphylococcus aureus* PC1 at 2.0 Å resolution. J. Mol. Biol. 217:701–719, 1991.
9. Knox, J.R., Moews, P.C. β-lactamase of *Bacillus licheniformis* 749/C. Refinement at 2 Å resolution and analysis of hydration. J. Mol. Biol. 220:435–455, 1991.
10. Jelsch, C., Lenfant, F., Masson, J.M., Samama, J.P. β-lactamase TEM1 of *E. coli:* Crystal structure determination at 2.5 Å resolution. FEBS Lett. 299:135–142, 1992.
11. Herzberg, O., Kapadia, G., Blanco, B., Smith, T.S., Coulson, A. Structural basis for the inactivation of the P54 mutant of β-lactamase from *S. aureus* PC1. Biochemistry 30:9503–9509, 1991.
12. Knox, J.R., Moews, P.C., Escobar, W.A., Fink, A.L. A catalytically-impaired class A β-lactamase: 2 Å crystal structure determination and kinetics of the *Bacillus licheniformis* E166A mutant. Protein Eng. 6:11–18, 1993.
13. Strynadka, N.C.J., Adachi, H., Jensen, S.E., Johns, K., Sielecki, A., Betzel, C., Sutoh, K., James, M.N.G. Molecular structure of the acyl-enzyme intermediate in β-lactam hydrolysis at 1.7 Å resolution. Nature (Lond.) 359:700–705, 1992.
14. Matagne, A., Misselyn-Bauduin, A.M., Joris, B., Erpicum, T., Granier, B., Frère, J.M. The diversity of the catalytic properties of class A β-lactamases. Biochem. J. 265:131–146, 1990.
15. Jelsch, C., Lenfant, F., Masson, J.M., Samama, J.P. Crystallization and preliminary crystallographic data on *E. coli* TEM1 β-lactamase. J. Mol. Biol. 223:377–380, 1992.
16. Herzberg, O., Moult, J. Bacterial resistance to β-lactam antibiotics: Crystal structure of β-lactamase from *Staphylococcus aureus* PC1 at 2.5 Å resolution. Science 236:694–701, 1987.
17. Crowther, R.A. The fast rotation function. In: "The Molecular Replacement Method." Rossmann M.G. (ed) New York; Gordon and Breach, 1972: 173–178.
18. Crowther, R.A., Blow, D.M. A method of positioning a known molecule in an unknown crystal structure. Acta Crystallogr. 23:544–548, 1967.
19. Sussman, J.L. Constrained-restrained least-squares (CORELS) refinement of proteins and nucleic acids. Methods Enzymol. 115:271–303, 1985.

20. Brünger, A.T. X-PLOR Manual, v. 2.1. The Howard Hughes Medical Institute and Department of Molecular Biophysics and Biochemistry, Yale University, New Haven, CT, 1990.
21. Jones, T.A. A graphics model building and refinement system for macromolecules. J. Appl. Crystallogr. 11:268–272, 1978.
22. Bricogne, G. Methods and programs for direct-space exploitation of geometric redundancies. Acta. Crystallogr. A32:832–847, 1976.
23. Hendrickson, W.A. Stereochemically restrained refinement of macromolecular structures. Methods Enzymol. 115:252–270, 1985.
24. James, M.N.G., Sielecki, A.R. Structure and refinement of penicillopepsin at 1.8 Å resolution. J. Mol. Biol. 163:299–361, 1983.
25. Luzatti, V. Traitement statistique des erreurs dans la détermination des structures cristallines. Acta Crystallogr. 5:802–810, 1952.
26. Kabsch, W., Sanders, C. Dictionary of protein secondary structure: Pattern recognition of hydrogen bonded and geometrical features. Biopolymers 22:2577–2637, 1983.
27. Richardson, J.S. The anatomy and taxonomy of protein structure. Adv. Protein Chem. 34:167–339, 1981.
28. Leszinski, J.F., Rose, G.D. Loops in globular proteins: A novel category of secondary structure. Science 234:849–855, 1986.
29. Murphy, B.P., Pratt, R.F. Evidence for an oxyanion hole in serine β-lactamases and DD-peptidases. Biochem. J. 256: 669–672, 1988.
30. Christensen H., Martin, M.T., Waley, S.G. β-lactamases are fully efficient enzymes. Biochem. J. 266:853–861, 1990.
31. Dalbadie-McFarland, G., Neitzel, J.J., Richards, J.H. Active site mutants of β-lactamase: Use of an inactive double mutant to study requirements for catalysis. Biochemistry 25:332–338, 1986.
32. Schulz, S.C., Dalbadie-McFarland, G., Neitzel, J.J., Richards, J.H. Stability of wild type and mutant RTEM-1 β-lactamases: Effect of disulfide bond. Proteins 2:290–297, 1987.
33. Palzkill, T., Botstein, D. Probing β-lactamase structure and function using random replacement mutagenesis. Proteins 14:29–44, 1992.
34. Delaire, M., Labia, R., Samama, J.P., Masson, J.M. Site-directed mutagenesis of *E. coli* TEM-1 β-lactamase. J. Biol. Chem. 267:20600–20606, 1992.
35. Healey, W.J., Labgold, M.R., Richards, J.H. Substrate specificities in class A β-lactamases: Preference for penams vs. cephems. The role of residue 237. Proteins 6:275–283, 1989.
36. Jacob-Dubuisson, F., Lamotte-Brasseur, J., Dideberg, O., Joris, B., Frère, J.M. Arginine 220 is a critical residue for the catalytic mechanism of the *Streptomyces albus* G β-lactamase. Protein Eng. 4:811–819, 1991.
37. Samraoui, B., Sutton, B.J., Todd, R.J., Artymiuk, P.J., Waley, S.G., Phillips, D.C. Tertiary structural similarity between a class A β-lactamase and a penicillin-sensitive D-alanyl carboxypeptidase-transpeptidase. Nature (Lond.) 320:378–380, 1986.
38. Adachi, H., Ohta, T., Matsuzawa, H. Site-directed mutants, at position 166, of RTEM-1 β-lactamase that form a stable acyl-enzyme intermediate with penicillin. J. Biol. Chem. 266:3186–3191, 1991.
39. Delaire, M., Lenfant, F., Labia, R., Masson, J.M. Site-directed mutagenesis on TEM1 β-lactamase: Role of Glu166 in catalysis and substrate binding. Protein Eng. 4:805–810, 1991.
40. Lenfant, F., Labia, R., Masson, J.M. Replacement of lysine 234 affects transition state stabilization in the active site of β-lactamase TEM1. J. Biol. Chem. 266:17187–17194, 1991.
41. Zafarella, G., Manavathu, E.K., Lerner, S.A., Mobashery, S. Elucidation of the role of Arg244 in the turnover processes of class A β-lactamases. Biochemistry 31:3847–3852, 1992.
42. Moews, P.C., Knox, J.R., Dideberg, O., Charlier, P., Frère, J.M. β-lactamase of *Bacillus licheniformis* 749/C at 2 Å resolution. Proteins 7:156–171, 1990.
43. Neu, H.C. The crisis in antibiotic resistance. Science 257: 1064–1073, 1992.